catalysts

MDPI

Communication

A Novel Synthetic Route to Prepare High Surface Area Mayenite Catalyst for TCE Oxidation

Adriano Intiso [1], Joaquin Martinez-Triguero [2], Raffaele Cucciniello [1], Antonio Proto [1], Antonio Eduardo Palomares [2,*] and Federico Rossi [1,3,*]

1 Department of Chemistry and Biology, University of Salerno, via Giovanni Paolo II 132, 84084 Fisciano (SA), Italy; aintiso@unisa.it (A.I.); rcucciniello@unisa.it (R.C.); aproto@unisa.it (A.P.)
2 Instituto de Tecnología Química, Universitat Politècnica de València-CSIC, 46022 Valencia, Spain; jomarti@itq.upv.es
3 Department of Earth, Environmental and Physical Sciences (DEEP Sciences), University of Siena, Pian dei Mantellini 44, 53100 Siena, Italy
* Correspondence: apalomar@iqn.upv.es (A.E.P.); federico.rossi2@unisi.it (F.R.); Tel.: +34-963877007 (A.E.P.); +39-0577235738 (F.R.)

Received: 27 November 2018; Accepted: 24 December 2018; Published: 1 January 2019

Abstract: Mayenite ($Ca_{12}Al_{14}O_{33}$) was synthesized by a novel route based on the use of polymethyl methacrylate (PMMA) as a soft templating agent. The material was tested for the total oxidation of trichloroethylene in the gas phase and the catalytic performance was analysed when using different initial amounts of PMMA in the catalyst synthesis. The results were compared with those obtained with a mayenite synthetized by a classical hydrothermal method. The highest activity in terms of TCE conversion was achieved in the presence of mayenite prepared using 10% *w*/*w* of PMMA; its activity was also higher than that of the hydrothermal mayenite. The surface area and the number of superoxide anions (O_2^-) seem to be the main properties determining the catalytic activity of the material.

Keywords: Mayenite; TCE; PMMA; catalytic oxidation

1. Introduction

Mayenite ($Ca_{12}Al_{14}O_{33}$, C12A7) is a mesoporous calcium aluminate that recently has attracted many researchers from different fields of chemistry, with applications ranging from passive sampling to steam reforming [1–6]. The physical properties of mayenite are correlated to its crystalline structure. In particular, $Ca_{12}Al_{14}O_{33}$ presents a cubic structure that may be described as a network of interconnected cages with a positive electric charge per unit cell, (I-43d with lattice parameters, a = 11.989 Å, α = β = γ = 90, Z = 2), expressed as $[Ca_{24}Al_{28}O_{64}]^{4+}$. The electroneutrality condition is fulfilled by the presence of two oxide ions, O^{2-} (free oxygen), trapped in the cages [6]. The high mobility of the free oxygen at high temperatures is a peculiar property of the mayenite exploited for many applications, including hydrogen storage, catalysis, fuel cells, oxidation of organic molecules, and electron conduction [7–13].

Among all the different routes proposed to synthesize mayenite, a solid-state reaction between $CaCO_3$ and Al_2O_3 (1200/1350 °C, 24/48 h) is the first and the most commonly used [14]. The as-obtained mayenite generally shows a very low surface area (~1 m^2/g) and a low porosity (pore volume ~0.01 cm^3/g). Wet chemistry routes have been recently developed to synthesize mayenite with improved physicochemical properties in terms of porosity, surface area, and number of O_2^- reactive species. In this scenario, the citrate sol-gel method was proposed by Ude et al. [15], wherein highly porous mayenite was obtained using $Ca(NO_3)_2{\cdot}4H_2O$, $Al(NO_3)_3{\cdot}9H_2O$ and citric

acid as starting materials. Furthermore, Li and co-workers [16] described a new synthetic method, namely hydrothermal, that allowed the production of mayenite with a high porosity (pore volume ≈ 0.1 cm^3/g) and surface area (>20 m^2/g), exploiting lower calcination temperatures (about 600 °C). Catalyst's surface area is an important parameter for oxidative processes of organic compounds in heterogeneous catalysis, as demonstrated, for example, by Solsona et al. in the decomposition of propane on CuO-CeO_2-based catalysts [17]. Solsona and coworkers employed PMMA as a soft templating agent during catalyst preparation for increasing their surface area, thus improving the oxidation yield of propane [17]. In a previous work, we reported the influence of the synthesis method on mayenite activity for the trichloroethylene (TCE) oxidation [18]. In particular, hydrothermal, ceramic, and sol-gel routes were employed for the synthesis of the mayenite and we found that the hydrothermal method yielded the material with the best catalytic performances due to an optimum combination of surface area and redox properties.

Nevertheless, the surface area of the material is still quite low and it is expected that an increase of this parameter will result in a better activity of the material. In this work, mayenite was prepared through a novel synthetic route based on the use of different amounts of PMMA (10–20% *w*/*w*), with the aim of improving the physico-chemical properties of the catalyst. The performance of the synthesized catalysts was then evaluated for the oxidation of TCE in the gas phase, the latter chosen as a probe for chlorinated volatile organic pollutants [19]. Light-off curves showed that mayenite synthesized using 10% *w*/*w* PMMA was the most effective in the TCE oxidation reaction. Catalysts were characterized by means of XRD, BET, and Raman techniques to define the structure, the surface area, and the presence of the free oxygen, respectively.

2. Results and Discussion

Figure 1 reports the XRD pattern of mayenite prepared using 10% *w*/*w* of PMMA during the synthesis (mayenite 10), while patterns of the other materials are reported in the Supporting Materials (Figure S3). Together with the major phase, mayenite ($Ca_{12}Al_{14}O_{33}$, **Δ**), an additional phase of calcite ($CaCO_3$, ●) was detected. The formation of this phase was most probably a consequence of the reaction between the CO_2 produced by the template combustion and unreacted CaO [6], as it occurs with the Ca-based materials used for carbon dioxide absorption [20,21]. $CaCO_3$ amount was quantified as ~10 wt % by thermogravimetric analyses (see Figure S2 in the Supporting Materials). A similar pattern was obtained for Mayenite 20.

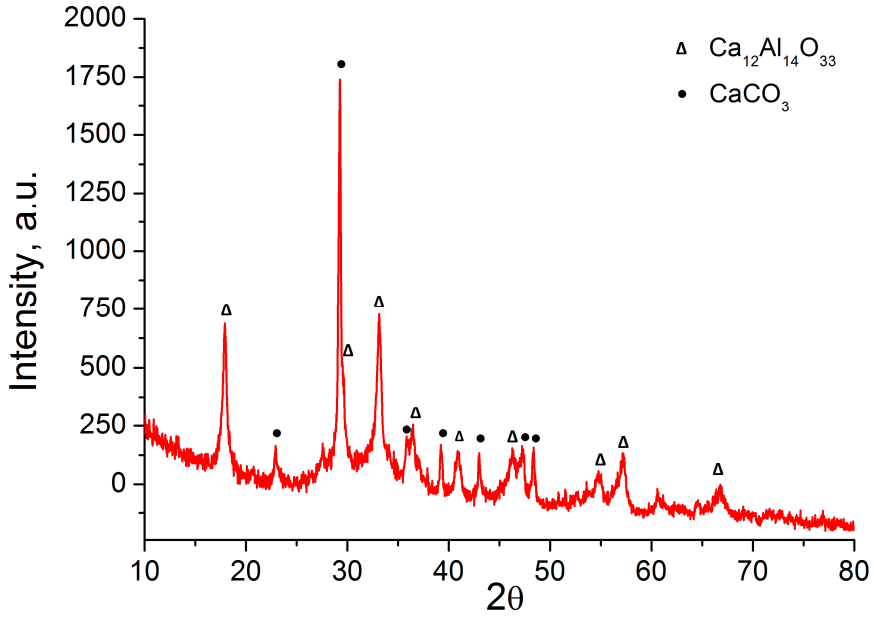

Figure 1. XRD pattern of mayenite 10.

The textural properties of the synthesized catalysts are reported in Table 1. Pure mayenite (mayenite) prepared in the absence of PMMA showed a BET surface area of 35.5 m^2/g in line with data reported for hydrothermal synthesis of mayenite [16]. Mayenite synthesized with 10% *w*/*w* of PMMA (Mayenite 10) showed the highest BET surface area, whilst increasing the template agent by other 10% (mayenite 20) resulted in a BET decrease from 47.1 to 41.9 m^2/g. The increase of the surface area was accompanied by a decrease of the total porosity of the material, as also evidenced by FESEM images reported in the Supporting Materials (Figure S5).

Table 1. BET surface area of the different synthesized catalysts.

Catalyst	BET Surface Area (m^2/g)	Total Pore Volume (cm^3/g)	Pore Diameter (nm)
Mayenite	35.5	0.252	11.88
Mayenite 10	47.1	0.183	8.98
Mayenite 20	41.9	0.183	9.00

The presence of free oxygen was investigated by means of Raman spectroscopy on the sample with the highest surface area and compared with pure mayenite. Both spectra (Figure 2) showed the presence of characteristic superoxide anions (O_2^-), the catalytic active species of mayenite for oxidation reactions [7,22,23], at a frequency of 1085 cm^{-1} [24]. Considering that both materials have the same chemical composition and hence they are optically similar, a rough comparison of the signals corresponding to superoxide anions showed that the presence of PMMA during the catalyst synthesis increased the number of free oxygens trapped into the mayenite structure, thus potentially enhancing its catalytic activity.

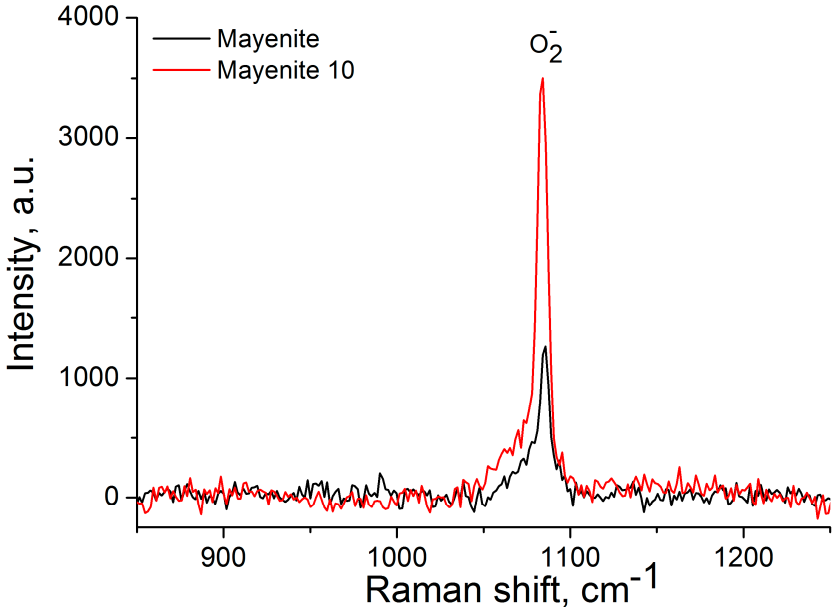

Figure 2. Raman spectra of mayenite (black) and mayenite 10 (red) catalysts.

The performances of the synthesized catalysts were evaluated by monitoring the trichloroethylene conversion as a function of the temperature (light-off curve). Figure 3 reports the conversion curve for mayenite 10 and 20 in comparison with mayenite used as the reference material [25].

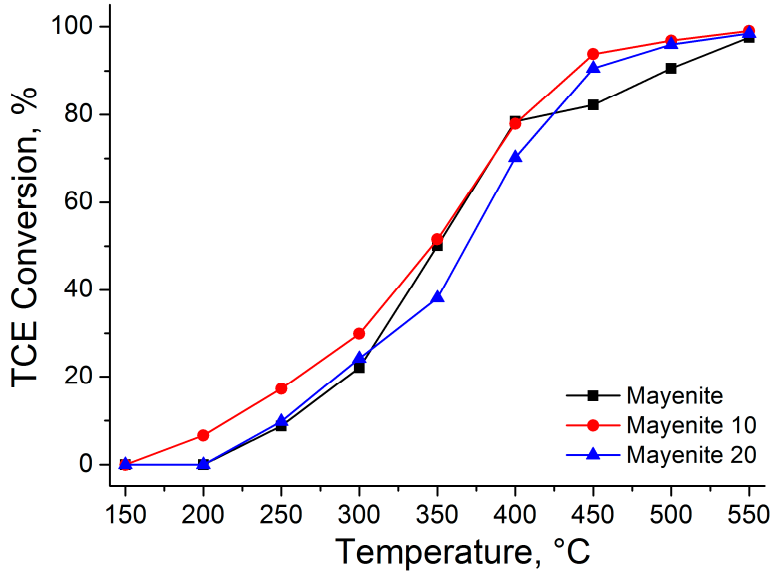

Figure 3. TCE conversion under wet conditions for mayenite (black), mayenite 10 (red), and mayenite 20 (blue). (catalyst = 0.7 g, [TCE] = 1000 ppm, water vapour = 1.7%, flux = 400 mL/min, GHSV = 12,000 h^{-1}).

Although there was not a significant improvement of the activity of mayenite 10 compared with the mayenite prepared without PPMA at temperatures higher than 550 °C, the activity of mayenite 10 at lower temperatures was much better than that of mayenite. In fact, at T = 200 °C, mayenite 10 oxidized (8% of conversion) TCE whereas mayenite and mayenite 20 were still inactive. T_{50} and T_{90} were lower for mayenite 10 (350 °C and 440 °C, respectively), whilst for mayenite and mayenite 20, they were 350/490 °C and 370/450 °C, respectively. These results are very interesting because industry needs active catalysts at low temperatures to minimize operational costs. The improved activity of mayenite 10 could be related to the surface area and O_2^- concentration. Thus, to prepare an active mayenite-based catalyst for the TCE oxidation, an optimum combination of surface area and oxidative properties was required. Blank experiments were performed without catalyst and no significant conversion (<10%) was observed in the temperature interval of 150–550 °C. Products' distribution analyses showed that the main TCE oxidation products were CO_2, CO, and HCl, in line with previous studies [18,26–28].

A stability test was also performed to compare the activity of mayenite 10 and mayenite (Figure 4).

Initially, mayenite 10 was more active and stable than mayenite, whereas a moderate deactivation process occurred after 2 h of reaction for both catalysts. To clarify the deactivation mechanism, XRD patterns of mayenite 10 were recorded before and after the catalytic oxidation (see Figure S4 Supporting Materials). The results revealed the disappearance of the $CaCO_3$ phase; then, we can speculate that calcium carbonate impurities could be responsible for the initial enhancement of mayenite 10 stability due to the reaction between $CaCO_3$ and in-situ produced HCl (TCE oxidation product), with the formation of a well dispersed $CaCl_2$ phase [18,25,27]. It is difficult to provide here a thorough characterization of this neutralization process, however, calcite formation was strictly related with the presence of the templating agent during mayenite synthesis and this basic phase easily reacted with the acid molecule of HCl; in contrast, in materials synthetized with different methods (hydrothermal, ceramic, and sol-gel [18]), and after the disappearance of $CaCO_3$ in mayenite 10, HCl generated during the TCE oxidation could only react with the anionic oxygen species (O_x^{x-}), causing the formation of chloromayenite (brearleyite), with the consequent deactivation of the catalyst [18,25,27].

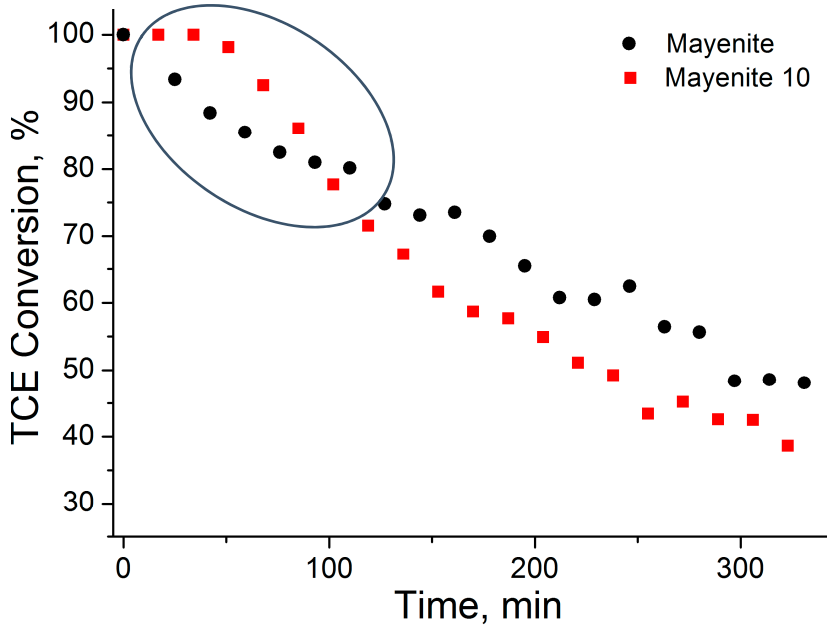

Figure 4. Stability curves for mayenite (black circles) and mayenite 10 (red squares) catalysts (catalyst = 0.7 g, [TCE] = 1000 ppm, water vapour = 1.7%, flux = 400 mL/min, GHSV = 12,000 h^{-1}, T = 500 °C).

3. Materials and Methods

3.1. Catalyst Preparation

Hydrothermal mayenite was prepared by following the method described by Li et al. [16]: 41.5 g of $Ca(OH)_2$ (95% from Sigma-Aldrich, St. Louis, MO, USA; no. 239232) and 50.7 g of $Al(OH)_3$ (95% from Sigma-Aldrich, no. 239186) were mixed in 1 L of milli-q water and ground to a powder under magnetic stirring for 4 h at room temperature. Afterwards, the mixture was placed in a stainless-steel autoclave and introduced in an oven pre-heated at 150 °C for 5 h. The obtained solid was filtrated and dried at 120 °C overnight (12 h), crushed into fine powder, and placed into a furnace at 600 °C in air for 4 h. The material was cooled at room temperature in a dry environment.

PMMA-based mayenite was synthesized by following a similar procedure, but 10 and 20 wt % of polymer (ESPRIX technologies, Sarasota, FL, USA; MX-series 150) were mixed with a stoichiometric amount of $Ca(OH)_2$ (41.5 g) and $Al(OH)_3$ (50.7 g), stirred in 1L of distilled water, and ground to a powder. Then, they were placed in a teflon-lined stainless-steel autoclave at 150 °C for 5 h. The solid was recovered by filtration and dried at 120 °C overnight (12 h). The following calcination ramp was applied: (1) 2.6 °C/min from room temperature up to 500 °C in N_2 atmosphere; (2) 500 °C for 4 h in N_2 to remove PMMA (see also Figure S1 in the Supporting Materials); (3) 1.7 °C/min from 500 °C to 600 °C in air; (4) 600 °C in air for 4 h to form the mayenite phase. The material was cooled at room temperature in a dry environment. The water content of the material was estimated to be around 5% by TGA measurements (see Supporting Materials for details).

Materials were named as mayenite X, where X corresponds to the amount of PMMA added during the synthesis, i.e., 10 (10% *w*/*w* of PMMA) and 20 (20% *w*/*w* of PMMA).

3.2. Characterization of Mayenite Catalyst

X-ray diffraction patterns were obtained by using an X'Pert-Pro diffractometer (Panalytical, Amsterdam, The Netherlands) equipped with an X'Celerator detector and using Ni-filtered Cu K radiation. The step size was 0.04° with a step time of 35 s. The BET surface areas were determined on an ASAP 2010 instrument (Micromeritics Corp., Norcross, GA, USA) using nitrogen as the

probe molecule at liquid nitrogen temperature (−196 °C). The samples (300 mg) were pretreated with vacuum at 400 °C and the BET method was used to calculate the surface area. The Raman spectroscopy experiments were carried out using a Horiba Jobin Yvon-Labram HR UV-visible-NIR Raman Spectrometer (Kyoto, Japan), using a 514 nm wavelength laser for excitation. Spectra were recorded averaging 10 scans obtained in different points of the sample at a resolution of 2 cm^{-1}. The microstructure of the catalysts, deposited as a thin monolayer, was investigated using a field emission scanning electron microscopy (FESEM) (Zeiss Ultra 55, Carl Zeiss, Oberkochen, Germany). TGA measurements were carried out using a thermogravimetric analyser (TA instruments, TGA Q500, New Castle, PA, USA) on 5 mg samples, over a temperature range from 25 °C to 900 °C, at a heating rate of 10 °C/min, under an inert atmosphere of nitrogen.

3.3. TCE Oxidation Reactions

Experiments were carried out in a home-made quartz fixed bed reactor, increasing the reaction temperature from 150 to 550 °C in steps of 50 °C. Silicon carbide (> 0.6 mm, Sigma-Aldrich) was placed above the catalyst (0.7 g) located on a quartz plug in the middle of the reactor. The inlet gas, composed by 1000 ppm of trichloroethylene (TCE, ACS reagent, >99.5%; Sigma-Aldrich, St. Louis, MO, USA) and synthetic air (N_2/O_2 80:20), was introduced into the reactor at 400 mL/min (Gas Hourly Space Velocity, GHSV = 12.000 h^{-1}) [28]. Water was injected in the inlet gases with a syringe pump, to obtain 1.7% *v*/*v* of water vapour in the gas flow. All details about the analytical procedures to evaluate the product distribution have been described in our previous work [18,25]. Blank experiments were performed at the same operative conditions without using catalyst, to assess the contribution of thermal oxidation. All measurements were repeated three times to assure the reproducibility of the results. In all the experiments, the error analysis of triplicate results was under 5%.

4. Conclusions

In this work, mayenite catalyst was prepared by a novel synthetic route based on the use of PMMA as a soft templating agent and tested for the total oxidation of TCE. We have shown that by using this new method, an increase of the catalyst surface area of 35% can be obtained, increasing also the number of active sites (anionic oxygen). The increase of the surface area is essential to improve the catalytic activity of bulk materials as mayenite and we have shown that this material (mayenite 10) presented the best performance in terms of T_{10} and T_{90} (350 °C and 440 °C, respectively). The good performance of mayenite 10 was related to an optimum balance between the surface area and the amount of superoxide anions. TCE was totally converted in less harmful products, such as CO_2 and HCl, confirming our previous studies about products' distribution. Mayenite 10 showed also a slightly better stability with respect to mayenite, during the first hour of reaction. This material is then a cheap and effective VOC (Volatile Organic Compound) oxidation catalyst that can partially trap the HCl produced during the reaction.

From this work, we can conclude that it is possible to improve the catalytic properties of mayenite by modifying the synthesis method, thus obtaining a material with a higher surface area. This improvement can be exploited not only for the TCE oxidation, but also for other catalytic processes where mayenite is not generally employed because of its low surface area.

Supplementary Materials: The following are available online at http://www.mdpi.com/2073-4344/9/1/27/s1, Figure S1: Thermogram of pure PMMA; Figure S2: Thermogram of mayenite 10; Figure S3: XRD patterns of tested catalysts; Figure S4: XRD patterns of mayenite 10 before and after stability test; Figure S5: FESEM images of the mayenite and mayenite 10.

Author Contributions: Conceptualization, A.I., R.C., A.P. and F.R.; investigation, A.I. and J.M.-T.; resources, F.R., A.P. and A.E.P.; data curation, A.I., J.M.-T. and R.C.; writing—original draft preparation, A.I. and R.C.; writing—review and editing, F.R. and A.E.P.; supervision, F.R., A.P. and A.E.P.

Funding: This research was funded by University of Salerno, grant number ORSA167988 and ORSA174250.

Acknowledgments: A.I. gratefully acknowledges the Erasmus + traineeship program. Authors are also in debt with Jesus Gracia Soguero for technical assistance.

Conflicts of Interest: The authors declare no conflict of interest. The funders had no role in the design of the study; in the collection, analyses, or interpretation of data; in the writing of the manuscript, or in the decision to publish the results.

References

1. Fujita, S.; Ohkawa, M.; Suzuki, K.; Nakano, H.; Mori, T.; Masuda, H. Controlling the Quantity of Radical Oxygen Occluded in a New Aluminum Silicate with Nanopores. *Chem. Mater.* **2003**, *15*, 4879–4881. [CrossRef]
2. Sushko, P.V.; Shluger, A.L.; Hayashi, K.; Hirano, M.; Hosono, H. Mechanisms of oxygen ion diffusion in a nanoporous complex oxide $12CaO{\cdot}7Al_2O_3$. *Phys. Rev. B* **2006**, *73*, 014101. [CrossRef]
3. Matsuishi, S.; Toda, Y.; Miyakawa, M.; Hayashi, K.; Kamiya, T.; Hirano, M.; Tanaka, I.; Hosono, H. High-Density Electron Anions in a Nanoporous Single Crystal: $[Ca_{24}Al_{28}O_{64}]^{4+}(4e^-)$. *Science* **2003**, *301*, 626–629. [CrossRef] [PubMed]
4. Kamiya, T.; Aiba, S.; Miyakawa, M.; Nomura, K.; Matsuishi, S.; Hayashi, K.; Ueda, K.; Hirano, M.; Hosono, H. Field-Induced Current Modulation in Nanoporous Semiconductor, Electron-Doped $12CaO{\cdot}7Al_2O_3$. *Chem. Mater.* **2005**, *17*, 6311–6316. [CrossRef]
5. Baptista, M.; Kovalevsky, A.V.; Sarabando, A.R.; Ferro, M.C.; Capela, I.; Frade, J.R. Highly-porous mayenite-based ceramics by combined suspension emulsification and reactive sintering. *Mater. Lett.* **2019**, *237*, 41–44. [CrossRef]
6. Cucciniello, R.; Proto, A.; Rossi, F.; Motta, O. Mayenite based supports for atmospheric NO_x sampling. *Atmos. Environ.* **2013**, *79*, 666–671. [CrossRef]
7. Li, C.; Hirabayashi, D.; Suzuki, K. A crucial role of O_2^- and O_2^{2-} on mayenite structure for biomass tar steam reforming over $Ni/Ca_{12}Al_{14}O_{33}$. *Appl. Catal. B Environ.* **2009**, *88*, 351–360. [CrossRef]
8. Huang, J.; Valenzano, L.; Sant, G. Framework and Channel Modifications in Mayenite ($12CaO{\cdot}7Al_2O_3$) Nanocages By Cationic Doping. *Chem. Mater.* **2015**, *27*, 4731–4741. [CrossRef]
9. Kitano, M.; Inoue, Y.; Yamazaki, Y.; Hayashi, F.; Kanbara, S.; Matsuishi, S.; Yokoyama, T.; Kim, S.-W.; Hara, M.; Hosono, H. Ammonia synthesis using a stable electride as an electron donor and reversible hydrogen store. *Nat. Chem.* **2012**, *4*, 934–940. [CrossRef] [PubMed]
10. Hayashi, F.; Tomota, Y.; Kitano, M.; Toda, Y.; Yokoyama, T.; Hosono, H. NH_2^- Dianion Entrapped in a Nanoporous $12CaO{\cdot}7AlO_3$ Crystal by Ammonothermal Treatment: Reaction Pathways, Dynamics, and Chemical Stability. *J. Am. Chem. Soc.* **2014**, *136*, 11698–11706. [CrossRef]
11. Ruszak, M.; Witkowski, S.; Sojka, Z. EPR and Raman investigations into anionic redox chemistry of nanoporous $12CaO{\cdot}7Al_2O_3$ interacting with O_2, H_2 and N_2O. *Res. Chem. Intermed.* **2007**, *33*, 689–703. [CrossRef]
12. Ruszak, M.; Inger, M.; Witkowski, S.; Wilk, M.; Kotarba, A.; Sojka, Z. Selective N_2O Removal from the Process Gas of Nitric Acid Plants Over Ceramic $12CaO{\cdot}7Al_2O_3$, Catalyst. *Catal. Lett.* **2008**, *126*, 72–77. [CrossRef]
13. Proto, A.; Cucciniello, R.; Genga, A.; Capacchione, C. A study on the catalytic hydrogenation of aldehydes using mayenite as active support for palladium. *Catal. Commun.* **2015**, *68*, 41–45. [CrossRef]
14. Lacerda, M.; Irvine, J.T.S.; Glasser, F.P.; West, A.R. High oxide ion conductivity in $Ca_{12}Al_{14}O_{33}$. *Nature* **1988**, *332*, 525–526. [CrossRef]
15. Ude, S.N.; Rawn, C.J.; Peascoe, R.A.; Kirkham, M.J.; Jones, G.L.; Payzant, E.A. High temperature X-ray studies of mayenite synthesized using the citrate sol-gel method. *Ceram. Int.* **2014**, *40*, 1117–1123. [CrossRef]
16. Li, C.; Hirabayashi, D.; Suzuki, K. Synthesis of higher surface area mayenite by hydrothermal method. *Mater. Res. Bull.* **2011**, *46*, 1307–1310. [CrossRef]
17. Solsona, B.; Sanchis, R.; Dejoz, A.M.; García, T.; Ruiz-Rodríguez, L.; López Nieto, J.M.; Cecilia, J.A.; Rodríguez-Castellón, E. Total Oxidation of Propane Using CeO_2 and $CuO\text{-}CeO_2$ Catalysts Prepared Using Templates of Different Nature. *Catalysts* **2017**, *7*, 96. [CrossRef]
18. Intiso, A.; Martinez-Triguero, J.; Cucciniello, R.; Rossi, F.; Palomares, A.E. Influence of the synthesis method on the catalytic activity of mayenite for the oxidation of gas-phase trichloroethylene. *Sci. Rep.* **2018**. [CrossRef]
19. Cucciniello, R.; Proto, A.; Rossi, F.; Marchettini, N.; Motta, O. An improved method for BTEX extraction from charcoal. *Anal. Meth.* **2015**, *7*, 4811–4815. [CrossRef]

20. Broda, M.; Müller, C.R. Synthesis of Highly Efficient, Ca-Based, Al_2O_3-Stabilized, Carbon Gel-Templated CO_2 Sorbents. *Adv. Mater.* **2012**, *24*, 3059–3064. [CrossRef] [PubMed]
21. Cucciniello, R.; Proto, A.; Alfano, D.; Motta, O. Synthesis, characterization and field evaluation of a new calcium-based CO_2 absorbent for radial diffusive sampler. *Atmos. Environ.* **2012**, *60*, 82–87. [CrossRef]
22. Yang, S.; Kondo, J.N.; Hayashi, K.; Hirano, M.; Domen, K.; Hosono, H. Formation and Desorption of Oxygen Species in Nanoporous Crystal $12CaO{\cdot}7Al_2O_3$. *Chem. Mater.* **2004**, *16*, 104–110. [CrossRef]
23. Teusner, M.; De Souza, R.A.; Krause, H.; Ebbinghaus, S.G.; Belghoul, B.; Martin, M. Oxygen Diffusion in Mayenite. *J. Phys. Chem. C* **2015**, *119*, 9721–9727. [CrossRef]
24. Fujita, S.; Nakano, H.; Suzuki, K.; Mori, T.; Masuda, H. Oxidative Destruction of Hydrocarbons on $Ca_{12}Al_{14-x}Si_x\ O_{33+0.5x}$ ($0 \leq x \leq 4$) with Radical Oxygen Occluded in Nanopores. *Catal. Lett.* **2006**, *106*, 139–143. [CrossRef]
25. Cucciniello, R.; Intiso, A.; Castiglione, S.; Genga, A.; Proto, A.; Rossi, F. Total oxidation of trichloroethylene over mayenite ($Ca_{12}Al_{14}O_{33}$) catalyst. *Appl. Catal. B Environ.* **2017**, *204*, 167–172. [CrossRef]
26. Intiso, A.; Cucciniello, R.; Castiglione, S.; Proto, A.; Rossi, F. Environmental Application of Extra-Framework Oxygen Anions in the Nano-Cages of Mayenite. In *Advanced Bionanomaterials*; Springer: Cham, Switzerland, 2018; pp. 131–139. [CrossRef]
27. Schmidt, A.; Lerch, M.; Eufinger, J.-P.; Janek, J.; Tranca, I.; Islam, M.M.; Bredow, T.; Dolle, R.; Wiemhöfer, H.-D.; Boysen, H.; et al. Chlorine ion mobility in Cl-mayenite ($Ca_{12}Al_{14}O_{32}Cl_2$): An investigation combining high-temperature neutron powder diffraction, impedance spectroscopy and quantum-chemical calculations. *Solid State Ion.* **2014**, *254*, 48–58. [CrossRef]
28. Blanch-Raga, N.; Palomares, A.E.; Martínez-Triguero, J.; Valencia, S. Cu and Co modified beta zeolite catalysts for the trichloroethylene oxidation. *Appl. Catal. B Environ.* **2016**, *187*, 90–97. [CrossRef]